

PHY385: Experimental Investigations with Polarizers and Waveplates

Natalia Tabja
(Dated: February 2025)

We experimentally investigated the behavior of polarized light passing through linear polarizers and waveplates (quarter-wave and half-wave plates). By measuring transmitted light intensities via a photodiode for different polarizer orientations, we verified Malus' Law and demonstrated how waveplates alter the beam's polarization. A quarter-wave plate (QWP) between crossed polarizers only partially recovered light intensity, whereas a half-wave plate (HWP) could fully rotate the beam's polarization to match the analyzer. Finally, reflections from a dielectric surface were studied, examining how the incident polarization and angle of incidence affected the reflected intensity.

INTRODUCTION

Polarization is a key property of light describing the orientation of its electric field. Linear polarizers selectively transmit one polarization component, while waveplates (retarders) impose a phase shift between two orthogonal components, modifying the polarization state. Malus' Law predicts how two polarizers oriented at an angle θ reduce transmitted intensity by a factor of $\cos^2(\theta)$, and Jones calculus provides a matrix formalism to model polarizing elements and waveplates.

In this lab, we first examine simple two-polarizer configurations to confirm Malus' Law. We then insert a quarter-wave plate (QWP) or half-wave plate (HWP) between crossed polarizers to explore how each waveplate alters the beam's polarization and thus the transmitted intensity. Finally, we investigate how reflection from a glass surface depends on the incident polarization and angle of incidence, connecting our observations to Fresnel reflection coefficients and Brewster's angle.

POLARIZERS

Part (a): Observing Light Through Two Polarizers

When rotating the polarizers with respect to each other, there was a gradual decrease in light intensity, reaching a minimum when the polarizers were presumably around 90° relative to each other based on Malus' Law, where transmitted intensity follows

$$I = I_0 \cos^2(\theta),$$

where θ is the angle between the polarizers. As the angle was increased beyond this point, the intensity gradually increased, reaching maximum brightness when the polarizers were aligned (0° or 180°). The transition between maximum and minimum intensity was smooth, confirming that the polarizers were functioning correctly.

Parts (b-c): Experimentally Verifying Malus' Law

A Helium-Neon (HeNe) laser ($\lambda = 633$ nm) was used as the light source for this experiment. The laser beam was directed and aligned using two mirrors to ensure it reached the photodiode detector after passing through a set of two polarizers, as shown in Figure 1 and Figure 2.

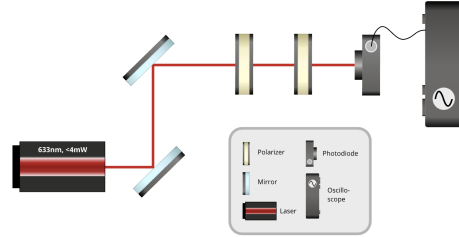


FIG. 1: Schematic diagram of the experimental setup used to verify Malus' Law. The laser beam passes through two linear polarizers before reaching the photodiode detector, allowing measurement of transmitted intensity as a function of relative polarizer angle.



FIG. 2: Photograph of the experimental setup for verifying Malus' Law. The HeNe laser beam is directed through two adjustable linear polarizers.

To prevent saturation of the photodiode, we adjusted the first polarizer until the maximum voltage recorded

(in the absence of the second polarizer) was 9.00 V on the oscilloscope. This value was set as our artificial maximum intensity reference. Furthermore, the background intensity was measured to be approximately 200 mV, which we subtracted from all voltage measurements to minimize systematic error.

We fixed the first polarizer at an angle of $304^\circ \pm 1^\circ$ in its rotary mount. The second polarizer was then rotated, starting at $114^\circ \pm 1^\circ$, in 5° increments up to 205° , recording the voltage on the oscilloscope at each step. We started with the second polarizer at $114^\circ \pm 1^\circ$ since this is where we found the maximum voltage to be recorded on the oscilloscope ($V_{\max} = 6.6 \pm 0.2$ V). The voltage uncertainty was calculated based on the oscilloscope's specifications:

$$\begin{aligned} \text{Gain accuracy} &= 2.0\% \times 8\text{V} = 0.16\text{V}, \\ \text{Resolution term} &= 0.2\% \times 8\text{V} = 0.016\text{V}. \end{aligned}$$

$$\implies \Delta V = 0.16\text{V} + 0.016\text{V} = 0.176\text{V} \approx 0.2\text{V}.$$

Since this exceeds observed fluctuations (± 0.1 V), we take $\Delta V = \pm 0.2$ V. In order to analyze the combined effects of the polarizers, the relative angle between them, θ_{rel} , was calculated as

$$\theta_{\text{rel}} = \theta_2 - \theta_1,$$

where θ_2 is the angle of the second polarizer, and θ_1 is that of the first. The uncertainty (to 1 s.f.) is

$$\Delta\theta_{\text{rel}} = \sqrt{(\Delta\theta_1)^2 + (\Delta\theta_2)^2} = \sqrt{1^2 + 1^2} = \sqrt{2} \approx 1^\circ.$$

Theoretical Derivation via Jones Matrices

In order to evaluate the experimental results, we can use the Jones matrix for a linear polarizer at angle θ :

$$P(\theta) = \begin{pmatrix} \cos^2 \theta & \sin \theta \cos \theta \\ \sin \theta \cos \theta & \sin^2 \theta \end{pmatrix}.$$

Taking the axis of the first polarizer as 0° , light emerging from it is

$$\mathbf{E}_1 = \begin{pmatrix} E_0 \\ 0 \end{pmatrix}.$$

If the second polarizer is at a relative angle θ_{rel} , it has Jones matrix $P(\theta_{\text{rel}})$. After passing through the second polarizer,

$$\mathbf{E}_2 = P(\theta_{\text{rel}}) \mathbf{E}_1 = \begin{pmatrix} \cos^2 \theta_{\text{rel}} E_0 \\ \cos \theta_{\text{rel}} \sin \theta_{\text{rel}} E_0 \end{pmatrix}.$$

The transmitted intensity, proportional to $|\mathbf{E}_2|^2$, is

$$I_2 = I_0 \cos^2(\theta_{\text{rel}}),$$

which is precisely Malus' Law.

Experimental Results & Analysis

As seen in Figure 3, the fitted $\cos^2(\theta)$ curve closely follows the experimental data, as indicated by a reduced chi-squared value of $\chi_r^2 = 1.12$. Furthermore, almost all data points fall within their respective uncertainty ranges, except for the data point at $\theta_{\text{rel}} = -164^\circ$, which deviates slightly. This suggests an overall agreement with Malus' Law.

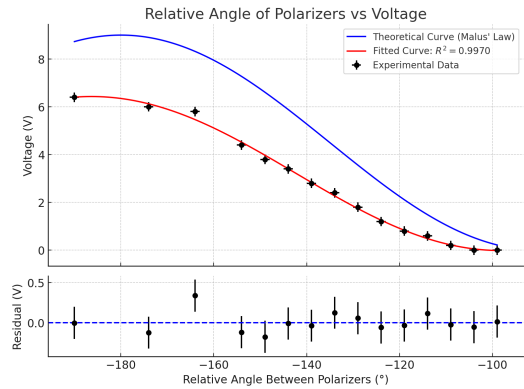


FIG. 3: Measured voltage as a function of relative polarizer angle. The best-fit curve follows Malus' Law: $V(\theta) = (6.45 \pm 0.15) \cos^2((1.02 \pm 0.01)\theta + (10.15 \pm 0.5)) + (-0.01 \pm 0.02)$ V. The reduced chi-squared value is $\chi_r^2 = 1.12$, indicating a good fit. The blue curve represents the theoretical expectation.

If we consider the coefficients of the fitted curve, we see that the coefficient $b = 1.02$ for the angle θ is very close to the expected value of 1.0. The coefficient $c = 10.15$ is likely due to the initial misalignment between the rotary mount's markings and the polarizer's true axis, as discussed earlier. This systematic offset does not affect the validity of Malus' Law but is an artifact of the experimental setup. Moreover, the offset term $d = -0.01$ V may be due to having removed the background noise from the measurements.

The coefficient a , or amplitude $I_0 = 6.45$ V, however, is only about 72% of our artificial $V_{\max} = 9.00 \pm 0.2$ V that was set using the first polarizer. This indicates that, despite the polarizers being aligned to transmit the highest possible intensity, potential imperfections or minor misalignments reduced the maximum light throughput. Real polarizers often have less than 100% transmission for the "aligned" polarization component, and any slight birefringence or contamination on their surfaces can further lower measured intensity.

WAVEPLATES

Parts (a-b): Quarter-Wave Plate Experiment

We initially set up the two polarizers so that their relative angle was 90° , ensuring minimal transmitted intensity ($\approx 0.2V$). The first polarizer was fixed at 304° , and the second at 205° . Inserting a quarter-wave plate (QWP) between them and adjusting the QWP angle in 5° increments allowed us to explore how the phase retardation affects the transmitted intensity through these “crossed” polarizers.

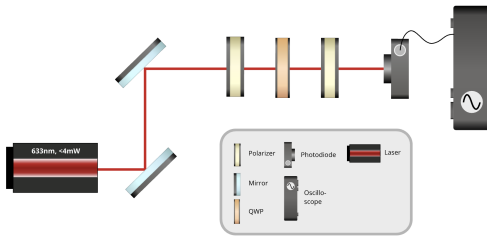


FIG. 4: Schematic diagram of the waveplate experiment setup. A laser beam passes through a linear polarizer, a waveplate (either QWP or HWP), and a second polarizer before being detected, allowing measurement of polarization-dependent intensity variations.



FIG. 5: Photograph of the experimental setup used to investigate the effect of waveplates on polarized light.

Theoretical Derivation via Jones Matrices

Take the light from the first polarizer as purely horizontal,

$$\mathbf{E}_1 = \begin{pmatrix} E_0 \\ 0 \end{pmatrix}.$$

A quarter-wave plate at angle θ has the Jones matrix

$$Q(\theta) = \begin{pmatrix} \cos^2 \theta + i \sin^2 \theta & (1-i) \sin \theta \cos \theta \\ (1-i) \sin \theta \cos \theta & \sin^2 \theta + i \cos^2 \theta \end{pmatrix}.$$

Thus,

$$\mathbf{E}_2 = Q(\theta) \mathbf{E}_1 = E_0 \begin{pmatrix} \cos^2 \theta + i \sin^2 \theta \\ (1-i) \sin \theta \cos \theta \end{pmatrix}.$$

Finally, the second polarizer (at 90° relative to the first) is

$$P(90^\circ) = \begin{pmatrix} 0 & 0 \\ 0 & 1 \end{pmatrix},$$

so the output field is

$$\mathbf{E}_3 = P(90^\circ) \mathbf{E}_2 = E_0 \begin{pmatrix} 0 \\ (1-i) \sin \theta \cos \theta \end{pmatrix}.$$

The transmitted intensity I_{out} is proportional to the squared magnitude of $(1-i) \sin \theta \cos \theta$. Since $|1-i| = \sqrt{2}$,

$$I_{\text{out}} \propto 2 \sin^2 \theta \cos^2 \theta = \frac{1}{2} \sin^2(2\theta).$$

Hence, between crossed polarizers, the quarter-wave plate can yield at most $\frac{1}{2} I_0$, and the transmitted intensity follows a $\sin^2(2\theta)$ dependence on the QWP’s orientation.

Experimental Results & Analysis

Figure 6 shows our data for voltage vs. QWP angle, together with a best-fit $\sin^2(2\theta)$ curve. The fit yields a reduced chi-squared value of $\chi_r^2 = 1.08$, and all points lie within experimental uncertainties.

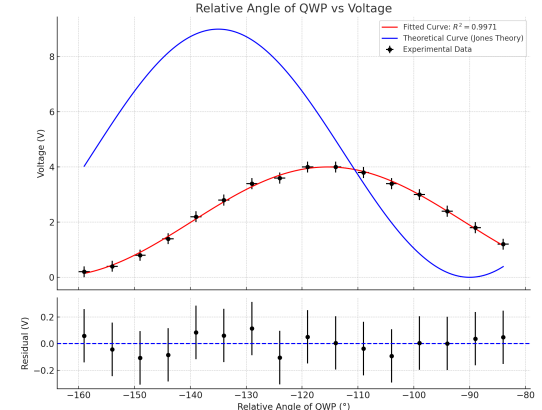


FIG. 6: Voltage measurements for a quarter-wave plate (QWP) placed between crossed polarizers. The best-fit curve follows:

$$V(\theta) = (4.00 \pm 0.12) \sin^2((2 \times (0.92 \pm 0.02)\theta + (122.89 \pm 0.8))) + (0.03 \pm 0.01) \text{ V}.$$

The reduced chi-squared value is $\chi_r^2 = 1.08$, demonstrating agreement with theoretical predictions from Jones calculus.

As before, we shall consider the coefficients of the fitted curve. First, we see that the coefficient $b = 0.92$ for the angle θ is very close to the expected value of 1.00. The coefficient $c = 122.89$ is far from the expected value of 0.00 for the same reasons as in the

two-polarizer system from before: the fast axis of the wave plate was not aligned with the 0° mark of the rotary mount, but rather $\approx 122.89^\circ$ away from it. Moreover, the offset term, $d = 0.03\text{V}$ is insignificant, and falls within the uncertainty ranges of the experiment.

From our first experiment using only two polarizers, we established that the maximum measured voltage when transmitting light through the first polarizer was 9V, when the polarizer was at $304 \pm 1^\circ$. This provides a reference for the incident intensity on the waveplate: $I_{\text{in}} \propto 9\text{V}$. Based on the theoretical calculations using Jones matrices, the maximum recorded voltage should have been half the original 9.0V, so around 4.5V, which is just over our experimental maximum of 4.0V. The small discrepancy is likely due to a combination of experimental factors. Aside from the factors discussed in section 2.3, imperfections in the waveplate's birefringence could have led to incomplete polarization transformation, reducing the transmitted intensity. Additionally, small misalignments of the waveplate's fast axis with respect to both the first and second polarizers could have caused loss in the total transmitted intensity. In particular, misalignment with the first polarizer could result in an incorrect phase shift, while misalignment with the second polarizer could cause the analyzed polarization state to deviate from the ideal case. Minimal losses due to material absorption, surface reflections, and coating inefficiencies in the optical elements may have further contributed to the smaller voltage that was recorded.

Part (c): Half-Wave Plate Experiment

For this part of the lab, we swapped the QWP for a HWP in the rotary mount, placing it at an initial 300° , as this was the angle at which we recorded a minimum voltage of 0.4V. We rotated the HWP in 10° increments and recorded the voltage on the oscilloscope at each step. The setup was identical to that seen in Figures 4 and 5, aside from the type of wave plate used.

Theoretical Derivation via Jones Matrices

A half-wave plate (HWP) at angle θ to the horizontal has Jones matrix

$$H(\theta) = \begin{pmatrix} \cos 2\theta & \sin 2\theta \\ \sin 2\theta & -\cos 2\theta \end{pmatrix}.$$

Again let the light from the first (horizontal) polarizer be

$$\mathbf{E}_1 = \begin{pmatrix} E_0 \\ 0 \end{pmatrix}.$$

Applying $H(\theta)$:

$$\mathbf{E}_2 = H(\theta) \mathbf{E}_1 = \begin{pmatrix} \cos(2\theta) E_0 \\ \sin(2\theta) E_0 \end{pmatrix}.$$

Then the second polarizer is oriented at 90° relative to the first:

$$P(90^\circ) = \begin{pmatrix} 0 & 0 \\ 0 & 1 \end{pmatrix}.$$

Hence,

$$\mathbf{E}_3 = P(90^\circ) \mathbf{E}_2 = \begin{pmatrix} 0 \\ \sin(2\theta) E_0 \end{pmatrix}.$$

The intensity is $\sin^2(2\theta) I_0$, which *can* reach the full incident intensity I_0 if $\theta = 45^\circ$. Physically, a half-wave plate at 45° simply rotates horizontal polarization by 90° , aligning it perfectly with the second polarizer's axis.

Experimental Results & Analysis

We found that inserting a half-wave plate between two crossed polarizers could indeed yield a higher maximum voltage (closer to the two-polarizer maximum of about 6.5 V), illustrating that a HWP can rotate linear polarization into the vertical direction, whereas the QWP cannot achieve a full 90° rotation of linear polarization.

Figure 7 compares our experimental measurements, the best-fit model, and an ideal half-wave-plate prediction. The best-fit function agrees with the data very well, yielding a reduced chi-squared value of $\chi_r^2 = 1.05$.

If we consider the coefficients of the fitted curve once more, we see that the coefficient for θ (1.02) is extremely close to the expected value of 1.0, confirming that the HWP nearly doubles the input polarization angle (as theory requires). Furthermore, the phase offset (2.6°) indicates a small misalignment of the waveplate's fast axis relative to our nominal zero. The vertical offset ($\approx 0.23\text{ V}$) is relatively small and may be explained by experimental limitations and measurement uncertainties, likely reflecting minor background signals or incomplete extinction. The amplitude (≈ 4.89) is below the ideal 6.5 V of the ideal HWP curve, indicating that real-world imperfections (waveplate retardance errors, polarizer losses, etc.) reduce the maximum transmitted intensity, as we have seen in previous cases.

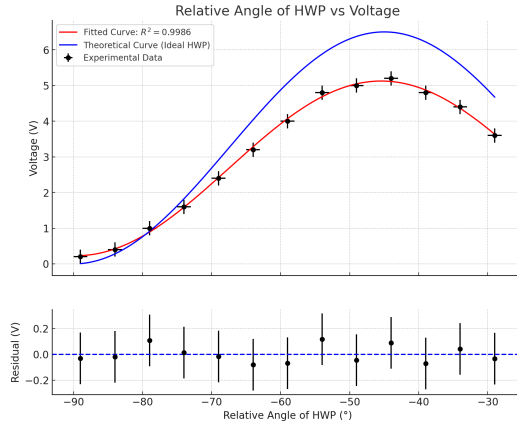


FIG. 7: Voltage measurements for a half-wave plate (HWP) between crossed polarizers. The best-fit model is:

$$V(\theta) = (4.89 \pm 0.10) \sin^2((2 \times (1.02 \pm 0.01)\theta + (2.60 \pm 0.4))) + (0.23 \pm 0.02) \text{ V}.$$

The reduced chi-squared value is $\chi_r^2 = 1.05$. The blue curve shows the ideal HWP case, where a full 90° rotation restores the maximum intensity.

Overall, while the $\sin^2(2\theta)$ behavior is clearly confirmed, the reduced peak voltage shows that practical limitations prevent the half-wave plate from perfectly rotating *all* of the incident light into the second polarizer's transmission axis.

d) Making Crossed Polarizers Transparent Using a Half-Wave Plate

Even when the two polarizers are crossed (i.e. oriented at 90° to each other) so as to pass a minimal amount of light, introducing a *half-wave plate* (HWP) at the appropriate angle can “unlock” the transmission. The HWP effectively *rotates* the linear polarization of the beam by 90° , realigning it with the second polarizer. In our experiment, although the nominal maximum transmission through two aligned polarizers was about 6.45 V, we obtained a peak of only 5.2 V with the HWP inserted between crossed polarizers. This shortfall from the expected value reflects practical imperfections such as non-ideal waveplate retardance, surface reflections, and finite polarizer efficiency.

e) Why a Quarter-Wave Plate Cannot Fully “Uncross” the Polarizers

By contrast, when we replaced the HWP with a *quarter-wave plate* (QWP), our maximum observed voltage was only about 4.0 V. This matches our theoretical analysis of a QWP between crossed polarizers, which shows at most half of the incident intensity can be transmitted, since a quarter-wave plate cannot simply rotate

linear polarization by 90° . Instead, it converts linear polarization into elliptical (or circular) polarization at certain orientations, and thus can never achieve the same complete “unlocking” that a half-wave plate can.

INVESTIGATING REFLECTIONS FROM A DIELECTRIC

Experimental Setup

As shown schematically in Fig. 8, we placed a polarizer and a half-wave plate (HWP) in the path of the laser beam so that we could produce a linearly polarized beam of any desired polarization angle. A glass window was then mounted at an oblique angle to reflect the beam onto the photodiode.

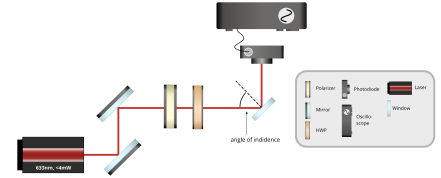


FIG. 8: Schematic diagram of the reflection experiment setup. The laser beam is polarized before striking a dielectric surface at an oblique incidence, with the reflected intensity measured by a photodiode.



FIG. 9: Photograph of the experimental setup for studying reflections from a dielectric surface.

(a) Arranging Polarization and Estimating the Angle of Incidence

We first placed a linear polarizer and a half-wave plate (HWP) before the beam to set a precise polarization angle. By rotating the HWP, one can produce any linear polarization ranging from purely *s*-polarized to purely *p*-polarized.

Here, ***s*-polarized** (or *perpendicular*) light refers to polarization where the electric field oscillates perpendicular to the plane of incidence—i.e., parallel to the reflecting surface. In contrast, ***p*-polarized** (or *parallel*) light has its electric field oscillating within the plane of incidence,

meaning it has a component along the direction of propagation of the incident and reflected rays.

A glass window was then mounted so that the beam struck it at an oblique angle, ϕ . By controlling the input polarization state, we could systematically investigate how the reflection behavior changes for different incident polarizations.

To estimate ϕ using trigonometry and the distance between holes on the breadboard as our units, we computed:

$$\theta = \arctan\left(\frac{2}{3}\right) \approx 34^\circ, \quad \phi = 90^\circ - \theta = 56^\circ.$$

This places us near Brewster's angle ($\theta_B \approx 56^\circ$) for glass with refractive index $n \approx 1.5$.

(b) Measuring the Reflected Intensity and Polarization

With the glass window fixed at $\phi \approx 56^\circ$, we aligned a photodiode to detect the beam reflected off the glass. By rotating the HWP (thus changing the incident beam's polarization), we recorded how much light was reflected for different polarization states. Table I shows our measured voltages for various HWP angles:

| HWP Angle (deg) | Incident Pol. (approx.) | Reflected Voltage (V) |
|-----------------|-------------------------|-----------------------|
| 0 | <i>p</i> -polarized | 2.6 |
| 10 | mostly <i>p</i> | 2.4 |
| 20 | mixed (<i>p/s</i>) | 3.2 |
| 30 | mixed | 4.0 |
| 40 | mostly <i>s</i> | 4.4 |
| 50 | <i>s</i> -polarized | 4.6 |

TABLE I: Reflected voltages measured at $\phi \approx 56^\circ$ for different HWP settings.

As predicted by the Fresnel equations, *p*-polarized light (in the plane of incidence) reflects less intensely than *s*-polarized light. Consequently, we observe a lower voltage at angles corresponding to near-*p* polarization (e.g. HWP near 0 – 10°) and a higher voltage for near-*s* polarization (around 40 – 50°).

(c) Effect of Angle of Incidence on Reflected Polarization

Although we planned to adjust the glass mount further and explore how the reflected polarization depends on ϕ ,

time constraints prevented us from completing this part of the experiment. Ideally, we would have measured the reflected intensity for a range of angles (e.g., $\phi = 30^\circ$ to 70°) and shown that at Brewster's angle ($\approx 56^\circ$ for glass), *p*-polarized light is minimally reflected. This leaves the reflection almost entirely *s*-polarized, meaning that the reflected beam is strongly linearly polarized.

For angles below Brewster's angle, both *s*- and *p*-components are reflected, but since there is no relative phase shift introduced between them, the reflected beam remains *linearly polarized*, just with a different polarization angle. At angles well above Brewster's angle, however, the reflection coefficients for *s*- and *p*-polarizations differ not only in magnitude but also in phase, causing the reflected beam to become *elliptically polarized*. This transition from linear to elliptical polarization as ϕ increases beyond Brewster's angle follows from the Fresnel equations, where the phase shift introduced for the *p*-component results in an elliptical polarization state.

Thus, while the reflected beam is always polarized, the distinction lies in whether the polarization remains linear (below Brewster's angle) or becomes elliptical (above it), depending on the relative phase difference between the reflected components.

CONCLUSION

Through a combination of experimental measurements and theoretical modeling, we confirmed Malus' Law for two polarizers, as our measured transmitted intensity followed the expected $\cos^2(\theta)$ dependence on the relative angle. Introducing a quarter-wave plate (QWP) between crossed polarizers never restored full transmission but instead reached at most half the original intensity, in agreement with Jones-calculus predictions that a QWP cannot rotate linear polarization by 90° . By contrast, replacing the QWP with a half-wave plate (HWP) allowed us to nearly recover the maximum intensity—further validating that a HWP can fully rotate linear polarization to match the analyzer. Finally, although we partially explored the reflection of polarized light from a dielectric at oblique incidence, time constraints limited our ability to map out the full dependence on angle. Nonetheless, our preliminary measurements were consistent with Fresnel equations and the concept of Brewster's angle, where *p*-polarized light is minimally reflected. Overall, these experiments underscore the utility of Jones calculus and basic polarization principles in explaining real-world optical measurements.